

Effect of focusing electric field on the formation of arc generated carbon nanotubes

Soumen Karmakar ^{1,5}, Harshada Nagar¹, R. Pasricha², T. Seth³, , V. G. Sathe⁴, S. V. Bhoraskar^{1,6} and A. K. Das⁵,

¹ Department of Physics, University of Pune, Pune 411 007, India

² National Chemical Laboratory, Pashan Road, Pune 411 008, India

³ Center for Materials for Electronics Technology, Panchawati, Pashan Road, Pune 411 008, India

⁴ UGC-DAE Consortium for Scientific Research, Indore Center, University Campus, Khandwa Road, Indore, 452 017, India

⁵ Laser and Plasma Technology Division, Bhabha Atomic Research Center, Trombay, Mumbai 400 085, India

⁶Corresponding author

Abstract

The effect of focusing electric field on the formation of carbon nano tubes in a direct-current arc-plasma is investigated. The hard deposits on the surface of the cathode are the main products, rich in multi-walled carbon nanotubes. It is seen that the focusing electric field has a distinct influence on the yield, purity and morphology of the nanotubes. A maximum yield of ~55 % of the total consumed anode material was obtained as carbon nanotubes. The deposition of amorphous carbon on the reactor wall reduced drastically on application of the focusing electric field. Transmission electron microscopy has been used to determine the morphology of the nanotubes. In addition, Raman spectroscopy has helped in distinguishing the nanotubes from the amorphous carbon and helped in analyzing the morphology of the tubes. Differential thermal analysis gave a clear feature of the useful yield of carbon nanotubes within the cathode-deposits. Crystalline nature of the nanotubes has been confirmed by X-ray diffraction analysis. The results clearly indicate that the focusing electric field confines the positively charged carbon precursors within the cathode-anode space causing high yield and purity and has a distinct effect on controlling the diameter of the as synthesized CNTs. The paper also discusses different aspects of the used characterization techniques before coming to any major conclusion related to mass.

1. Introduction

The discovery of carbon nanotubes (CNTs) has triggered a variety of research directions in application of this exotic material [1,2]. Some of the unique mechanical and electrical properties of carbon nanotubes have made them distinguished materials for considerable research right from their discovery. Various routes to synthesize CNTs [3,4] have well been established. Among all possible routes of synthesis of CNTs, arc-plasma method, is the simplest and oldest one and has perhaps been used most widely for their massive synthesizing ability [5,6]. However, this process is known to generate large amount of amorphous carbon and carbon particles with relatively less quantity of CNTs. The tubes obtained by this method were often riddled with defects and have a considerably lower aspect ratio as compared to the other synthesizing routes [7]. A number of attempts have been made to achieve better yield [8-11] and to avoid cumbersome purification processes that can cause damages to the as synthesized CNTs.

At present, higher percentage-yield and purity are of primary focus of research for using CNTs in reinforcing the polymer composites [12] and ceramics [13] or applying it to other areas like electrochemical double layer capacitors [14], solid hydrogen storage medium [15], field emissive displays [16], transistors [17], artificial actuators [18] etc.

One of the serious issues that has been plaguing the DC arc-generated CNTs is the low conversion due to considerable waste of the anode-material (as high as 90%) in the form of amorphous carbon (a-C) that diffuses out of the plasma zone and deposits on the walls of the reactor. There have been no attempts to find techniques to control this waste of the fed-material as a-C. The present study has examined the effect of focusing electric field on the efficiency of formation of CNTs in a direct current (DC) arc-plasma reactor. For the first time a high yield (~55 % of the total anode material consumed) of CNTs with minimum structural deformation has been achieved in the raw cathode-deposit (collaret). It is also extremely significant to note that the amount of CNTs within the collaret (under the application of focusing electric field) was about ~63 %, higher than figures cited by earlier researchers and is in contrast with the post purification figures often cited in the literature. Therefore, the simple but innovative application of focusing electric field has opened up tremendous possibility for bulk-production of CNTs.

The morphology of the as synthesized MWCNTs has been investigated using transmission electron microscopy (TEM); relative purity of the sample has been confirmed with the help of Laser Raman spectroscopy (LRS) and X-ray diffraction (XRD) analysis, whereas differential thermal analysis (DTA) has been employed to explore the percentages and thermal stabilities of different species present in the raw cathode-deposits. Finally, an attempt has been made to explore different possibilities behind the experimental outcomes.

2. Experimental details

A DC arc-plasma reactor, used for the synthesis of nano-phased materials [19-21], was specially modified for the production of carbon nanotubes in the present experiment. The schematic of this modified reactor is shown in figure 1.

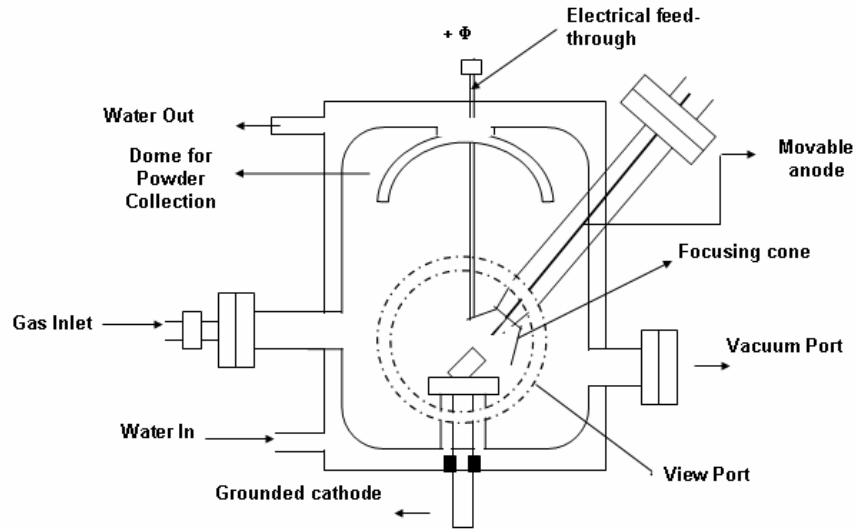


Figure 1: Schematic of the DC arc-plasma reactor.

Contrary to standard configuration [19-21], the upper and lower electrodes were made up of 99.99% pure graphite and served the purpose of anode and cathode respectively. A 4 kW DC power supply was used to ignite and maintain the arc discharge between the cathode ($\varphi=33$ mm) and the anode ($\varphi=10$ mm). The cathode was mounted at an angle of 45° with the substrate in order to make the axes of both the cylindrical electrodes co-linear. Figure 2 shows the three dimensional (3-D) view of the electrode assembly specially designed for this reactor.

Figure 2: 3-D view of the electrostatic focusing unit.

It consists of a truncated cone-shaped graphite anode electrically insulated from the main electrodes.

Initially, a base vacuum of 10^{-3} Torr was obtained in the reactor chamber by an oil-rotary vacuum pump. Then the chamber was filled with Ar-He mixture (40% Ar, 60% He by mole fraction) until a pressure of 500 Torr was achieved. The selection of the composition and pressure was as per the

experimental convenience. This pressure was kept constant throughout the experiment through a throttle valve. During the entire experiment the arc was run at a current of 100A and the inter electrode distance was always adjusted manually to maintain the anode to cathode voltage (ACV) fixed at 26 V. The focusing electrode was biased through a voltage regulated power supply of 2kV, 50mA rating. The cathode was grounded and all applied voltages were measured with respect to the ground. The experimental parameters are outlined in table1. Focusing voltage was maintained at 300V in order to keep the magnitude of the focusing electric field approximately twice of that in the arc roughly taking a 5mm separation between the main electrodes. This condition was chosen in order to make its contribution much higher than the thermal energy of the plasma precursors and to observe the profound effect of this on the formation dynamics of nanotubes. For each experiment the operational-time was restricted to 3 minutes.

Table 1: Specifications of operating parameters.

ACV (V)	26
Anode diameter (mm)	10
Cathode diameter (mm)	33
Arc current (A)	100
Focusing voltage ‘Φ’(V) applied during the first experiment	0V
Focusing voltage ‘Φ’(V) applied during the second experiment	300V
Operating chamber pressure (Torr)	500

Initially, CNT synthesis was carried out without applying any bias to the focusing electrode. The plasma was observed to be purple yellow in colour and was quite stable during the operation. At the end of operation, entire inner surface of the chamber was found to be covered by black carbon soot. When the focusing voltage was switched on, during the second operation, strong vortex near the cathode was observed and the plasma turned into greenish blue in colour. At the completion of this operation, the

carbon soot content was found to be drastically low on the reactor chamber wall. The experiments were repeated a number of times for confirmation.

After the completion of each synthesis-run, sufficient time was allowed to cool the interior of the chamber and then the hard deposits on the surface of the cathode were scraped off for characterization. The total mass losses of the anode and the collaret obtained were measured after each operation with the help of a sensitive digital balance (100 g capacity with least readability 10^{-4} g). After collection, the hard deposits were crushed in a pestle-mortar until they turned into fine black powder. For TEM analysis, the powders were dispersed in toluene ($C_6H_5-CH_3$) by mild sonication for one hour. This solution was stored untouched for 48 hours, so as to allow the graphitic impurities to settle down at the bottom of the sample bottle. The upper relatively clear portion of the solution was used for preparing the specimen on the carbon-coated copper grid for TEM investigations. For the other characterizations, the 'as is' fluffy powder was employed with no further processing. TEM investigation was done by employing JEOL 1200 EX microscope. Raman spectroscopy was carried out at room temperature with the help of JobinYvon HR800 spectrometer, whereas He-Ne LASER ($\lambda=632.81$ nm) was used for the Raman excitations. DTA was recorded in pure oxygen (O_2) ambience (flow rate = 50 cc/min i.e. 8.33×10^{-7} $m^3 s^{-1}$) by a METTLER TOLEDO STAR^e gravimeter. Crystalline structure was investigated by using PHILIPS 1866 X-ray Diffractometer with Cu-K_α line ($\lambda=1.542$ Å) as X-ray.

3. Results and discussions

The data generated from the experiment revealed some new and highly interesting results with respect to the mass of the collaret, the mass loss from anode, relative abundance of various allotropic forms of carbon (including CNT) and Raman excitations on application of the focusing electric field.

3.1 Fractional conversion: One of the major effects of the application of an electric field engulfing the arc zone is in the fractional conversion of anode mass in to the collaret. table 2 gives a summary of a typical measurement obtained under the two experimental conditions.

Table 2: Measurement of mass under the experimental conditions.

Bias condition	$\Phi = 0$ V	$\Phi = 300$ V
Mass of the total anode material consumed: M_A (mg)	386.2	362.9
Mass of the collaret: M_C (mg)	98.8	314.7
Conversion efficiency $\eta_{CD} = [M_C / M_A] \times 100\%$	25.6%	86.7%

The experiments have been repeated a number of times to rule out the possibility of any accidental outcome and the above-mentioned values of η_{CD} have been found to vary by 5%.

The conversion efficiency in the cathode deposit i.e. η_{CD} under $\Phi = 0$ V condition has been compared with the results of I. Hinkov et al [22]. While studying the effect of optimizing the anode cathode distance, Hinkov et al estimated η_{CD} to be $\sim 3\text{-}18\%$. This is in the same range of results shown in the second column of table 2. However, the efficiency of conversion of anode material to the collaret has increased dramatically ($\sim 240\%$) on applying the focusing voltage. This is highly encouraging and significant.

3.2 Raman spectroscopy: Another significant aspect of the effect of focusing electric field is seen in the Raman spectrum obtained for both the samples. Raman spectra were recorded at room temperature for the same samples by repeatedly exposing different portions of the samples for gathering the average feature. figure 3 shows the typical Raman spectra obtained from both the samples.

Figure 3: Raman spectra of CNTs synthesized at (a) $\Phi = 0$ V, (b) $\Phi = 300$ V.

These spectra show the presence of so-called disorder-induced D-band which appears near 1330 cm^{-1} . This band appears due to the presence of amorphous carbon in the sample. The tangential mode G, which is the typical characteristic of CNT, appears near 1582 cm^{-1} . The second order observed mode at 2650 cm^{-1} is assigned to the first overtone of the D mode and is often called as G' mode [23]. The comparison of the different bands can give an overview of the internal composition of the samples.

The Raman spectra for both the samples are identical except for a profound Raman peak at 278.9 cm^{-1} , the trace of which is totally absent in the sample corresponding to $\Phi = 0 \text{ V}$. This peak is a clear signature of the focusing electric field on the morphology of the as synthesized CNTs.

As reported by X. Zhao et al [24], this is a peak (reported value 279 cm^{-1}) that has often been observed for the multi-walled carbon nanotubes produced in H_2 atmosphere. However, until now nobody could ever observe this peak working with other atmosphere (e.g. He, Ar or their mixture). This peak indicates a marked difference in the morphology of the nanotubes produced under these experimental conditions. Ar-He atmosphere is known to generate CNTs, which have their inner diameters more than 2nm. As a result, nobody has ever observed radial breathing mode (RBM) for such tubes. However, the peak at 278.9 cm^{-1} is related to RBM of the tubes having 15 walls and inner diameter equal to 0.84nm [25].

The present study, therefore, rules out the criterion that H_2 is mandatory for such growth mechanism of CNTs. The comparison of the two Raman spectra in figure 3 clearly reveals that focusing electric field has a prominent impact on the growth of CNTs. It restricts the inner diameter of the tube from growing larger and regulates the wall thickness as well. The comparatively high intensity and narrow width of this peak confirms a considerable number of identical nanotubes within the corresponding sample. This, in turn, indicates higher structural homogeneity of the CNTs in the sample synthesized at $\Phi = 300 \text{ V}$ than those synthesized at $\Phi = 0 \text{ V}$.

3.3 TEM analysis: The effect of focusing electric field on the morphology of the samples has been studied using TEM. figure 4(a) shows the morphology of the products corresponding to zero bias condition.

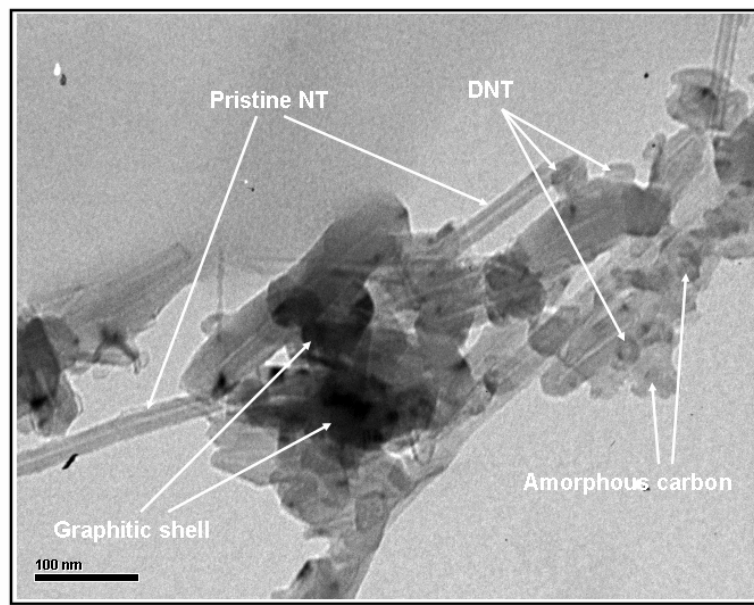


Figure 4(a): Transmission electron micrograph of the CNTs synthesized at $\Phi = 0$ V.

The figure shows large carbonaceous particles along with straw like CNTs having a wide outer-diameter distribution (10-50 nm). figure 4(b) shows a typical transmission electron micrograph of the products obtained on application of the focusing voltage.

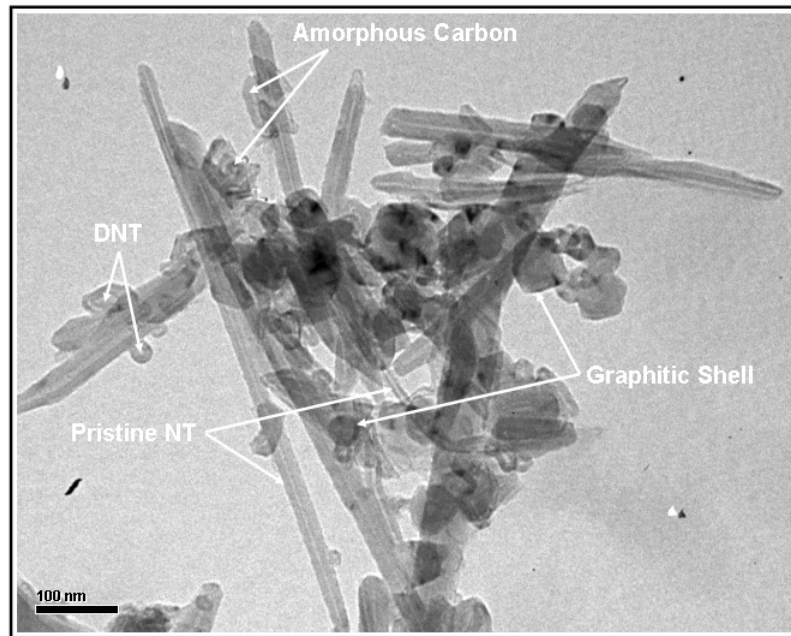


Figure 4(b): Transmission electron micrograph of the CNTs synthesized at $\Phi = 300$ V.

Here, relative abundance of CNTs is seen to have increased, the diameter distribution is narrower (15-25 nm) and the tubes are of longer lengths as compared to the previous case. In both the above two transmission electron micrographs the diameter and thickness of the tubes verifies their ‘multi-walled’ character.

No post-processing was carried out for the samples before recording the TEM images and therefore they obviously contain large amount of debris. This has been intentionally presented so as to highlight the effect of focusing electric field on reducing the content of debris in relation to that of carbon nanotubes. Moreover, at the present stage no attempts have been made to record the high resolution TEM images.

In this context, the focusing electric field regulates the growth of CNTs within the plasma zone with impact on their diameter distribution and possibly leads to higher relative yield. Traces of damaged tubes are also found to be present in both the micrographs.

However, it is emphatically noteworthy about few major complications while calculating mass from both TEM and LRS analysis. TEM represents two-dimensional micrographs of three-dimensional species which are spatially asymmetric in case of CNT containing samples generated by arc-discharge. Moreover, different species have different volume density of mass. So, to our belief, only relative numbers of the species along with their morphological insight are the only results, which can be concluded non-erroneously from TEM analysis. On the other hand, Raman peaks in the LRS analysis are associated with the type of the bonding and their relative numbers. The width of the Raman peaks is a measure of the degree of orderliness of the corresponding bonds. Although, these peaks contain information about the relative quantities of various allotropic forms of carbon, they do not provide the exact information about the relative masses.

3.4 Thermal investigation of the collaret composition: As has been discussed above (section 3.3), TEM alone cannot unambiguously quantify the amount of internal compositions of the as synthesized product. One of the reasons behind this is the ‘sampling (the way of choosing certain portion from the entire sample for a specific investigation)’. Predicting the purity and percentage (%) yield of CNTs with respect to mass within collaret from the TEM micrographs alone, therefore, is incongruous. It is therefore

necessary to support TEM data with information about the various degrees of crystallinity present in the product.

On the other hand, DTA is a much more realistic tool to investigate the samples both from qualitative as well as quantitative points of view. Although it responds to the ‘sampling’, still it shows overall behavior of the samples closer to the reality since it reflects the gross feature of the specimen.

Differential thermo gravimetry (DTG) is the commonly used technique for determining the degree of crystallinity in a sample through the investigation of rate of change of mass with temperature ($\delta m/\delta T$) [26]. However, the present study, for the first time, has used DTA, which additionally provides insight into the different crystalline phases exposing themselves during the process of oxidation. DTA was recorded in pure O₂ atmosphere for an amount of 3.2 mg of sample and the temperature difference was measured with respect to a standard alumina sample. Use of pure oxygen has a marked difference with the conventional thermal analysis techniques. The possibility of phase transition i.e. conversion of one allotrope of carbon to the other during the heating cycle in Ar or any other inert atmosphere having very less quantity (~5%) of oxygen can not be ruled out. As nanomaterials behave quite differently than their bulk counterpart, the above mentioned possibility is always there. On the other hand, pure oxygen atmosphere does not allow any allotropic conversion to happen except reacting with carbonaceous species to form gaseous CO₂. The area under the DTA curve is proportional to the mass of the sample [27] and DTA has the highest thermometric accuracy among all thermal processes, which use weighing of the mass [27]. It is therefore conjectured that calculation based on DTA under the present experimental circumstances is capable of producing results probably with best accuracy. Prominent signatures of all the species present in the sample are seen in the DTA curve (equivalent to reaction- rate Vs temperature curve) in figure 4(a, b). Reaction-rate was regulated by keeping the temperature ramp at 10°C/minute. Following the standard convention as applicable to the present case [25] the as recorded DTA envelop can be regarded to be a superimposition of four curves due to the presence of mainly four species viz. amorphous carbon (a-C), damaged nanotubes (DNT), structurally pure and defect-less pristine nanotubes (Pristine NT) and more thermally stable graphitic shells. These are the four main species those were seen present in the transmission electron micrographs (figure 4a, 4b). The percentage contribution of each

specie to the total mass (cathode-deposit) has been investigated by de-convoluting the DTA envelop into four different zones as shown in figure 5 (a) and 5(b).

Figure 5(a): The de-convoluted DTA curve obtained for the cathode-deposit synthesized at $\Phi = 0$ V. The Pi chart shows the percentage of different species present therein.

Figure 5(b): The de-convoluted DTA curve obtained for the cathode-deposit synthesized at $\Phi = 300$ V.

The Pi chart shows the percentage of different species present therein.

De-convolution is a purely mathematical procedure, which is always backed by the physical arguments. While obtaining de-convoluted graphs for both the DTA envelops, the number of the peaks was restricted to four. Keeping this number fixed, the peak position, width and area of the peaks were varied in a random fashion with a motivation to obtain the highest correlation coefficient between the fitted and the actual envelops. The above two figures represent the best fits thus obtained. We try to explain the possible inferences thus obtained.

Gaussian nature of the reaction profile for all the species was found to be most appropriate. A percentage contribution from different species has then been calculated on the basis of the area distribution as depicted in the same figure. It is noticeable that the peak position associated with a-C has been shifted from 250°C to 320°C under the application of the focusing field. Amorphous carbon (a-C) is a highly disordered network of carbon atoms with predominantly sp^2 bonds, with only approximately 10 % sp^3 bonds and no sp^1 bonds. a-C has no long-range order but only some short-range order ($\sim 10\text{\AA}$) that depends on the carbon bonding type (sp^2/sp^3) [28]. The sp^3 bond being stronger than sp^2 bond, it is difficult to oxidize it. Moreover, a-C assemblies have any kind of morphologies in shape, such as plate, sphere, polyhedron, droplet and cylinder with different orientations and sizes. This difference in structure is due to minimum surface tension and local discharge condition. The a-C peak shift indicates a change in

its internal composition and more sp^3 hybridized carbon-content in a-C under the action of electrostatic focusing.

The width of the peak in DTA is related to the degree of structural homogeneity of the corresponding specie. Lesser the width, higher is the structural homogeneity of the concerned specimen. In context to this, keeping in mind the logical inferences drawn from the LRS analysis, variable widths of peaks associated with different specimens present in the samples are expected.

It can, therefore, be concluded from the comparison of the two DTA curves that Pristine CNTs synthesized under the application of focusing electric field is more uniform in structure and thermally stable than its counterpart synthesized under no external bias. The relative abundance of pristine CNT is also more in the sample synthesized at $\Phi = 300$ V than that synthesized at $\Phi = 0$ V. These conclusions are consistent with the Raman spectroscopic analysis and the logical inferences drawn there from.

DTA analysis has been performed repeatedly, taking different parts of the same sample a number of times and the data presented here can be considered to consist of a maximum of $\pm 5\%$ error. The Pi charts glued in the figure 5(a) and 5(b) depict the relative change in the percentage of different species present in the two samples. Moreover, the positive value of ΔT in both the cases also signifies that the reaction of carbon species with oxygen is exothermic.

A good quantitative estimate of the conversion efficiency of total consumed anode-material into useful nanotubes can thus be obtained for the two experimental conditions as calculated in table 3.

Table 3: Calculation of conversion efficiency of fed anode material into CNTs.

Bias condition	$\Phi = 0$ V	$\Phi = 300$ V
Mass of the total anode material consumed: M_A from table1(mg)	386.2	362.9
Mass of the collaret: M_C from table1(mg)	98.8	314.7
% of CNTs within the collaret using DTA: P	42.1	63.2
Total mass of CNTs within the collaret: $M_C \times P = M_{CNT}$ (mg)	41.59	198.89

Conversion efficiency: $\eta_{\text{CNT}} = (M_{\text{CNT}} / M_{\text{A}}) \times 100\%$	10.7	54.8
---	------	------

The sixth row of table 6 reveals how the focusing electric field holds tremendous potential for converting a very large amount of fed material into useful nanotubes.

3.5 X-ray diffraction analysis: X-ray diffraction is one of the most commonly used techniques for examining the degree of crystallinity and phase of a material. Due to their intrinsic nature, the main features of X-ray diffraction pattern of CNTs are close to those of graphite (figure 6): (i) a graphite-like peak (002) is present and measurements of interlayer spacing can be obtained from its position using Bragg's law. (ii) A family of (h, k, 0) peaks is also present due to the honeycomb lattice of single graphene sheet.

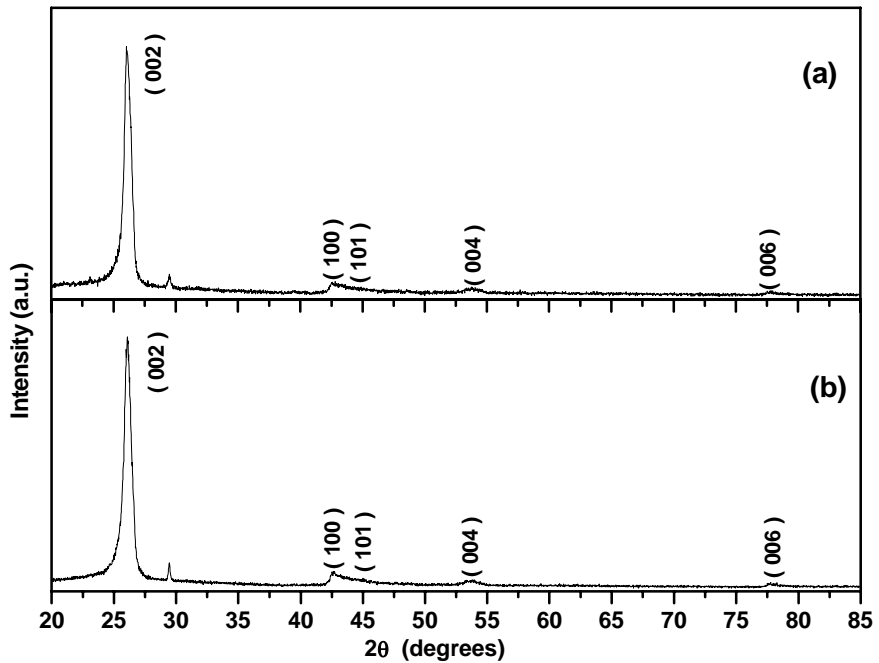


Figure 6: XRD pattern of the collaret synthesized at (a) $\Phi = 0$ V, (b) $\Phi = 300$ V.

Consequently, X-ray diffraction profile is not useful to differentiate multi-constructional details between the CNTs and the graphite structure [29] but can help to determine the sample purity. The XRD pattern

obtained for both the samples show good degree of purity and verifies the crystallinity of the samples. The XRD peak at $2\theta=26.4^\circ$ is a characteristic of graphite, wherein a shift of this pick towards $2\theta=26.00^\circ$ is attributed due to the presence of CNTs in the sample [29]. The observed peak at $2\theta=26.04^\circ$ and $2\theta=26.06^\circ$ for the two samples, therefore, verify the presence of carbon nanotubes in both the samples.

table 4 depicts the overall quantitative outcome of the present study.

Table 4. Comparative study of CNTs synthesized without and with the application of focusing

Voltage.

Bias condition	$\Phi = 0V$	$\Phi = 300V$
Inner diameter of the tubes (nm)	4-6	0.84-4
Outer diameter of the tubes (nm)	10 - 50	15 - 25
Average interlayer spacing of the tubes (\AA) (as calculated from XRD)	3.41	3.42
Most probable oxidation temperature of Pristine NT (K)	986	1003
Yield of Pristine NT in the collaret by mass (%)	8.5	24.3
Total yield of CNT in the cathode-deposit by mass (%)	42	63
Conversion efficiency of total fed anode material into useful nanotubes: η_{CNT} (%)	10.7	54.8

3.6 Effect of focusing electric field - A theoretical approach: The growth of carbon structures on a microscopic scale is governed by the attachment probabilities of carbon atoms, ions and clusters of

various sizes and shapes, controlled by a set of time and space-dependent parameters in the arc plasma formed in the inter-electrode region. Moreover, as a result of the random sputtering of the anode, the surface becomes irregular and the trajectories of the ejected species orient themselves randomly. In a region close to the cathode surface, the growth of carbon structures occurs due to the competitive input of groups of carbon species having different velocity distributions. An isotropic Maxwellian velocity distribution is thought to result in the formation of spherical carbon nanoparticles. On the other hand, if the velocity distribution becomes anisotropic, the reacting particles arrive in the reaction region in the form of a directed flux and conditions are created that are appropriate for creation of the elongated structures because of the formation of symmetry axes. [30,31]. The focusing electric field has the effect of directing the ion flux from the anode to the cathode quenching it towards the axis of the electrodes. Since the thermal energies are of the order of 0.3 – 1 eV, the field effect dominates over the thermal agitation. It is presumed that the randomness of electric field due to sputtering of the anode surface will not seriously alter the field lines.

To understand the effect of the focusing electric field, the distribution of electrostatic potential is essential. This can be found out by solving Poisson's equation

$$\nabla^2\Phi = \frac{\rho}{\epsilon} \quad (1)$$

for the used geometry and potentials of the electrodes.

where, Φ is the electrostatic potential, ρ is the volume density of charge and ϵ is the permittivity of the medium. However, it is well known that plasma is a quasi-neutral state of matter where the number of negative charge is same to that of the positive one. As a result, considering volume density of charge to be practically zero is a fairly good assumption. In lieu of this, Poisson's equation reduces to more simplified Laplace's equation given by

$$\nabla^2\Phi = 0 \quad (2)$$

Solutions of Laplace's equation can give comprehensive outline of the dynamics of charged particles that might take place during the formation of CNTs. In the regime of present experiments, Laplace's equation

has been solved using the boundary conditions as is described in figure7 with $\Phi=0V$ on the reactor chamber wall.

Figure7. Computational domain for solving Laplace's equation.

figure 8(a) shows the two-dimensional (2-D) view of equipotential lines originated from the two main electrodes when the focusing anode is grounded.

Figure 8(a): 2-D view of equipotential lines of the electrodes assembly when the focusing electrode is grounded.

The electric field is the negative of the gradient of the electrostatic potential and is always perpendicular to the equipotential lines. In context to this, a careful watch at figure 7(a) reveals that close to the outer edge of the two electrodes, positive ions have a tendency to fly away from the plasma zone. On the other hand, positive ions are forced to move in the vicinity of the plasma zone when focusing electrode is given a proper bias as shown in figure 8(b).

Figure 8(b): 2-D view of equipotential lines of the electrodes assembly with the focusing electrode biased at 300 Volt.

The effect of electrostatic field has in fact two-way actions. One component of the electric field is perpendicular to the actual current flow (E_{\perp}) and the other perpendicular to that (E_{\parallel}). E_{\perp} restricts the positively charged carbon precursors to leave the plasma zone and directs them towards the core of the plasma, which is responsible for the formation of nanotubes. On the other hand, E_{\parallel} assists in the deposition of the nanostructures on the cathode surface. As a result of this, the time of residence of positively charged carbon precursors within the plasma zone increases and so does the probability of

formation of CNTs. figure8(b) also explains unambiguously why under the application of focusing voltage almost no trace of carbon soot was found on the wall of the reactor chamber.

One important consideration that is likely to be addressed here is that during the synthesis process, cathode-deposit is formed in the form of cylindrical lump. This is likely to change the distribution of electrostatic potential discussed above. In both the experiments, therefore, run-time was restricted to only three minutes to avoid significant change in the efficiency of the focusing electric field. It is therefore predicted that a suitable measure has to be incorporated in the present apparatus to scrap out cathode-deposit during the synthesis process to run the experiments with same efficiency under the action of focusing electric field.

4. Summery and Conclusion

A novel idea of enveloping the region surrounding the arc by an electric field through a focusing electrode has yielded encouraging results. The yield of CNT is as high as $\sim 55\%$ of the mass of the total consumed anode material. A large amount of amorphous carbon being deposited on the chamber walls has, therefore, been eliminated. This is in high contrast with the conventional arc-plasma generators that wastes a very large amount (as high as 90%) of the total fed anode-material as amorphous carbon. The focusing electric field prevents the major loss of the fed material in the form of amorphous carbon and converts a significant amount of it into useful nanotubes. The focusing electric field also has a distinct role in regulating the diameter and thickness of the nanotubes. This phenomenon was supported by mass-measurement, Raman spectroscopy, transmission electron microscopy and differential thermal analysis. DTA has been successfully proved to be a useful tool to characterize CNT enriched samples from a compositional point of view.

For the first time the present experiment has clearly shown that Raman RBM peak at 279cm^{-1} can also be obtained without using H_2 as the compulsory buffer gas. The presence of H_2 is definitely not a mandatory criterion for such narrow inner diameter (0.84) of CNTs. This is a very crucial conclusion that definitely needs in-depth study.

The focusing field confines the charged particles to move along the lines of force. 300V focusing voltage for the present conditions and geometry bunches the positively charged plasma precursors

towards the axial position of the plasma and generates more profound directional motion in the cathode-anode space. Because of this, and since the thermal effects in charged-particles-collisions become negligible, the ions move in a co-current manner spending more time in the vicinity of each other. This, not only enhances the probability of agglomeration of the charged dust but trigger stacking in a specific direction. This leads to a highly non-equilibrium state leading to an environment conducive to attachment of carbon-groups more longitudinally than laterally during CNT formation.

One of the interesting observations related to the de-convoluted graph (figure 5.b) indicates the shift of the peak of amorphous carbon in DTA. This is a feature that definitely needs more detailed study and is being pursued.

In order to study the effect of more variation of the focusing electric field, the need of few modification of the reactor was felt. The work is in progress and being persuaded.

The simple but innovative application of focusing electric field has thus proved to have stupendous potential for exploring many hidden mystery of the frontier research related to nanoscience and nanotechnology.

Acknowledgements

The support from L&PTD, BARC, DAE, Government of India under the BARC-PU-MOU Collaborative research programme is gratefully acknowledged. S. Karmakar is grateful to NCL, Pune, C-MET, Pune and UGC-DAE-F, Indore, India, for giving opportunity to work with their characterizing tools and to all his lab-mates for constant support and encouragement. He would also like to thank Dr. V.K.Rohatgi for helpful and fruitful discussion. The support from Pune University Central Workshop, A Ahmed Al-Tabbakh and Dr. D.S.Joag is also specially acknowledged.

References

- [1] Iijima S
1991 Nature **354** 56-58
- [2] Endo M, Takeuchi K, Igarashi S, Kobori K, Shiraishi M and Kroto WH

1993 J Phys and Chem of Solids **54**(12)1841-48

[3] Thess A, Lee R, Nikolaev P, Dai H, Petit P, Robert J, Xu C, Lee YH, Kim SG, Rinzler AG, Colbert DT, Scuseria GE, Tománek D, Fischer JE and Smalley RE

1996 Science **273** 483-7

[4] Rao CNR, Govindaraj A, Sen R and Satishkumar BC

1998 Materials Research Innovations **2**(3)128-141

[5] Ebbesen TW and Ajayan PM

1992 Nature **358** 220-222

[6] Colbert DT, Zhang J, McClure SM, Nikolaev P, Chen Z, Hafner JH, Owens DW, Kotula PG, Carter CB, Weaver JH, Rinzler AG and Smalley RE

1994 Science **266** 1218-22

[7] Baddour CE and Briens C

2005 International Journal of Chemical Reactor Engineering Vol.**3R3**:1-22

[8] Ishigami M, Cumings J, Zettl A and Chen S

2000 Chem Phys Lett **319** 457–459

[9] Parkansky N, Boxman RL, Alterkop B, Zongtag I, Lereah Y and Barkay Z

2004 J Phys D: Appl Phys **37** 2715-19

[10] Anazawa K, Shimotani K, Manabe C and Watanabe H

2002 Appl Phys Lett 81(4)739-41

[11] Yao Y, Wang R, Wei DZ, Du D and Liang J

2004 Nanotechnology **15** 555-58

[12] Schadler LS, Giannaris SC and Ajayan PM

1998 Appl Phys Lett **73**(26) 3842-4

[13] Hwang GL and Hwang KC

2001 J. Mater. Chem. **11** 1722–1725

[14] Emmenegger CH, Mauron PH, Sudan P, Wenger P, Hermann V, Gallay R and Zuttle A

2003 Proceedings from Processing and Fabrication of Advanced Materials XI, ASM International pp. 408

[15] Pradhan BK, Harutyunyan AR and Stojkovic D
2002 J.Mater.Res.vol.**17** No.9

[16] Choi WB, Chung DS, Kang JH, King HY, Jin YW, Han IT, Lee YH, Jung JE, Lee NS, Park GS and Kim JM
1999 Appl Phys Lett **75**(20) 3129-31

[17] Tans SJ, Verschueren ARM and Dekker C
1998 Nature **393**(6680) 49-52

[18] Baughman RH, Cui C, Zakhidov AA, Iqbal Z, Barisci JN, Spinks GM, Wallace GG, Mazzoldi A, Rossi DD, Rinzler AG, Jaschinski O, Roth S and Kertesz M
1999 Science **284** 1340-4

[19] Balasubramanian C, Godbole VP, Rohatgi VK, Das AK and Bhoraskar SV
2004 Nanotechnology **15** 370

[20] Crescenzi MD, Castrucci P, Scarselli M, Diociaiuti M, Chaudhari PS, Balasubramanian C, Bhate TM and Bhoraskar SV
2005 Appl Phys Lett **86** 231901-03

[21] Madhukumar P, Balasubramanian C, Sali ND, Bhoraskar SV, Rohatgi VK and Badrinarayanan S
1999 Mater. Sci. and Eng. B. **63** 215

[22] Hinkov I, Farhat S, Chapelle MLDL, Fan SS, Han HX, Li GH and Scott CD
2001 NASA Proceedings *Optical plasma control during arc carbon nanotube growth*

[23] Keszler AM, Nemes L, Ahmed SR and Fang X
2004 Journal of Optoelectronics and Advanced Meterials **6**(4) 1269-74

[24] Zhao X, Ando Y, Qin LC, Kataura H, Maniwa Y and Saito R
2002 Chemical Physics Letters **361** 169–174

[25] Wang CY, Ru CQ and Mioduchowski A
2005 Journal of Applied Physics **97** 024310

[26] Nikolaev P

2005 *Purity measurement and purity standard of single-wall carbon nanotubes* 2nd Joint workshop on Measurement Issues in Single Wall Carbon Nanotubes: Purity and Dispersion Part II, January 26-28, NIST, Gaithersburg, MD

[27] Willard HH, Merritt LL, Dean JA and Settle FA

1986 *Instrumental Methods of Analysis* Seventh Edition, Wadsworth Publishing Company, USA p 766

[28] Bladh K, Falk LKL and Rohmund F

2000 *Appl. Phys. A* **70** (3) 317-322

[29] Belin T and Epron F

2005 *Mat. Sc. and Engg. B* **119** 105-118

[30] Charlier JC and Iijima S

2001 *Topics Appl. Phys.* **80** 55–81

[31] Bernholc J, Brabec C, Nardelli MB, Maiti A, Roland C and Yakobson BI

1998 *Appl. Phys. A* **67** 39–46